Available online at www.sciencedirect.com
ScienceDirect
Chinese Journal of Natural Medicines 2019, **17**(6): 0435–0445
Chinese Journal of Natural Medicines

Cimicifuga heracleifolia is therapeutically similar to black cohosh in relieving menopausal symptoms: evidence from pharmacological and metabolomics studies

MIAO Lan-Yun[1], CHU Thi Thanh Huyen[1], LI Ping[1], JIANG Yan[2*], LI Hui-Jun[1*]

[1] *State Key Laboratory of Natural Medicines, China Pharmaceutical University, Nanjing 210009, China;*
[2] *College of Chemical Engineering, Nanjing Forestry University, Nanjing 210037, China*

Available online 20 May, 2019

[ABSTRACT] In the market of botanical dietary supplements, *Cimicifuga heracleifolia* (CH) has always been considered as an adulterated species of *Cimicifuga racemosa* (CR), a conventional American herb with promising benefits to counteract troubles arising from the menopause. However, the detailed comparison of their therapeutic effects is lacking. In present study, the pharmacological and metabolomics studies were comparatively conducted between CH and CR in ovariectomized (OVX) female rats. Specifically, estrogen-like, anti-hyperlipidemia and anti-osteoporosis effects were evaluated through measuring serum biochemical parameters, histopathological examination and micro computed tomography (Micro-CT) scanning. At the same time, a gas chromatography-mass spectrometry (GC-MS)-based serum metabolomics method was employed to profile the metabolite compositional changes. As a result, both CR and CH displayed anti-osteoporosis and anti-hyperlipemia on menopause syndrome. Meanwhile, their potentials in improving the OVX-induced metabolic disorders were discovered. In conclusion, these results demonstrated that CH is therapeutically similar to CR in relieving menopausal symptoms and CH could be considered as a promising alternative to CR instead of an adulterant in the market of botanical dietary supplements.

[KEY WORDS] *Cimicifuga heracleifolia*; Black cohosh; Menopausal symptoms; Metabolomics; Substitute

[CLC Number] R965 **[Document code]** A **[Article ID]** 2095-6975(2019)06-0435-11

Introduction

Menopause is the time of life when menstrual cycles cease, resulting from reduced secretion of the ovarian hormones estrogen and progesterone [1]. Symptoms of menopause are characterized clinically by hot flushes, night sweats, vaginal atrophy and dryness [1-2]. Moreover, estrogen deficiency may relate to an increased risk of metabolic diseases, such as osteoporosis and hyperlipemia [3]. These conditions can be improved by hormone/estrogen replacement therapy (HRT/ERT), which is considered a first line choice for prevention of menopausal symptoms [4-5]. However, previous studies have acknowledged that HRT leads to the risks of breast cancer [6], endometrial cancer and heart attacks [7-8], which are generally called estrogen-like side effects. Therefore, non-hormone therapy is urgently needed in clinic.

In this context, many herbal medicines are developed to combat various menopausal symptoms. Among them, Remifemin® is a representative derived from *Cimicifuga racemose* (CR) (Fam. Ranunculaceae), an herbaceous perennial plant native to eastern North America. It is widely prescribed to help women counteract troubles arising from the menopause [9-10] in clinic for its hormonal-like action, without exhibiting estrogenic effects [11]. Actually, the roots and rhizomes of *C. racemose* (English name: black cohosh) have long been used medicinally by Native Americans, which are thought to possess analgesic, sedative, and anti-inflammatory properties [12-13]. Similarly, some Chinese *Cimicifuga* species also have long medicinal history. The rhizomes of *Cimicifuga heracleifolia* (CH), *C. dahurica*, and *C. foetida* are officially listed in Chinese pharmacopoeia (Chinese name: Sheng-Ma) [14], for the treatment of wind-heat headache, sore throat, toothache and uterine prolapse according to Chinese medicine theory.

[Received on] 22-Feb.-2019
[Research funding] This work was supported by the National Natural Science Foundation of China (Nos. 81773993 and 81130068) and the National Key R&D Program of China (No. 2018YFC-1707905).
[*Corresponding authors] Tel: 86-25-85427544, E-mail: jiangyan-cpu@126.com (JIANG Yan); Tel/Fax: 86-25-83271379, E-mail: cpuli@163.com (LI Hui-Jun)
These authors have no conflict of interest to declare.

Pharmacological researches have revealed that these Chinese species showed pronounced anti-osteoporosis effects [15-16]. Furthermore, phytochemical studies have demonstrated that 9, 19-cycloartane triterpenoids, a group of specific constituents responsible for various curative effects, are occurring in *Cimicifuga* taxa [17-18]. As described above, Chinese *Cimicifuga* species and black cohosh are genetically and chemically similar. Unfortunately, the formers are often considered as adulterants in the market of botanical dietary supplements [17, 19], albeit the comparison evaluation is lacking.

In order to efficiently explore the beneficial values of Chinese *Cimicifuga* species in the treatment of menopausal syndrome, the pharmacological and metabolomics studies were comparatively conducted between CH and CR in ovariectomized (OVX) female rats in present study.

Materials and Methods

Phytochemical study

Plant materials

The underground parts (roots and rhizomes) of *Cimicifuga heracleifolia* (CH) were purchased from Bozhou, Anhui Province, China, during July 2017. The original plant was authenticated by Prof. LI Hui-Jun, China Pharmaceutical University and the voucher specimen (No. 170103) was deposited in the State Key Laboratory of Natural Medicines, Nanjing, China. CH samples were cut into small pieces and refluxed with 60% (*V*/*V*) ethanol twice at a solid-liquid ratio of 1 : 10 for 2 h. The combined extracts were filtered. The filtrates were concentrated under reduced pressure to remove ethanol and then lyophilized. The final yield of the lyophilized CH powder was approximately 20%. The high performance liquid chromatography-evaporative light scattering detection (HPLC-ELSD) method was applied to determine major triterpenoid saponins in CH extract, revealing the contents of (23*R*, 24*S*) cimigenol-3- *O*-*β*-D-xylopyranoside (0.567%, *W*/*W*) and 24-*epi*-7, 8-didehydrocimigenol-3-*O*-*β*-D-xylopyranoside (0.799%, *W*/*W*). Before administration to rats, the lyophilized powder was re-dissolved and dispersed in ultrapure water.

Remifemin® tablets, purchased from Schaper & Brümmer GmbH & Co., KG (Salzgitter, Germany), were employed as standardized CR extract in our study. Each Remifemin tablet (0.28 g) corresponded to 20 mg of raw CR according to the specification. The tablets were ground into fine powders, and the powder was dissolved and dispersed in ultrapure water before use.

Chemical reagents

Methanol of chromatographic grade was provided by Tedia (Fairfield, USA). *N*-methyl-(trimethylsilyl) trifluoroacetamide (MSTFA), methoxyamine hydrochloride, pyridine and 2-isopropylmalic acid (internal standard, IS) were purchased from Sigma-Aldrich (Shanghai, China).

Animal experiments

Animal administration

All experiments and animal care were conducted in accordance with the Provision and General Recommendation of Chinese Experimental Animals Administration Legislation and were approved by the Science and Technology Department of Jiangsu Province (license number: SCXK (HU) 2013-0016). Forty healthy female Sprague Dawley (SD) rats (weight: 200 ± 20 g, 8-week-old) were provided by Sino-British Sippr/BK Lab Animal Ltd. (Shanghai, China). Before surgery, all rats were housed in the laboratory for 1 week to adapt to their surroundings. All rats were allowed free access to water and foods with a 12 h light and 12 h dark cycle. Considering the clinical practice of CR recommended by specifications, rats were treated with 60 mg·kg^{-1} CR or CH (i.e. 60 mg herbal drug/kg body weight). Moreover, we also designed another CH dosage according to Chinese Pharmacopoeia [14], 180 mg·kg^{-1} (i.e. 180 mg herbal drug/kg body weight), to evaluate its effect on menopausal syndrome. The experimental rats were randomly divided into following five groups: Sham-operated (Sham, n = 8), OVX-operated (OVX, n = 8), OVX-operated + CR (60 mg·kg^{-1}, n = 8), OVX-operated + CH low dose (CH-L) (60 mg·kg^{-1}, n = 8), OVX-operated + CH high dose (CH-H) (180 mg·kg^{-1}, n = 8). The administration started 2 weeks after surgery and lasted 12 weeks. Individual body weight was recorded weekly for adjustment of the drug dosage and food intake was measured weekly.

Biological sample collection and preparation

After 12 weeks of treatment, all experimental rats were fasted for 16 h and 1 mL of blood was collected from fundus venous plexus and left it to stand for 30 min, and then centrifuged at 3000 r·min^{-1} for 15 min at 4 °C. The supernatant was stored at –80 °C before used for biochemical analysis and GC-MS analysis. At the end of experiment, rats were sacrificed by decapitation to collect uterus tissues, intra-abdominal fat and femurs for analyzing the parameters. And then, the uterus (including vagina) and femur were removed from the surrounding connective tissues and muscles. The weights of these organs were measured for absolute wet-weights. The relative weights (% of body weight) were calculated, for reducing the individual differences.

Measurement of pharmacological parameters

Serum biochemical parameters

The levels of estradiol (E2), osteocalcin (OC), alkaline phosphatase (ALP), cross-linked carboxy-terminal telopeptide of type Ⅰ collagen (CTX-Ⅰ) and tartrate-resistant acid phosphatase 5b (TRACP 5b) were analyzed by ELISA kits (Biocalvin Co., Ltd, Suzhou, China). In addition, blood fat including serum total cholesterol (TC), triacylglycerol (TG), high-density lipoprotein cholesterol (HDL-c) and low-density lipoprotein cholesterol (LDL-c) were detected using assay kits (Jiancheng Bioengineering Institute, Nanjing, China).

Histopathological examination and Micro-CT scanning

Uterus specimens and abdominal fat pads were fixed in 10% buffered formalin solution at sacrifice. The right femur of each rat was separated, and then decalcified in decalcifying solution before being fixed in 10% buffered formalin solution. All the specimens were sectioned to 3–4 μm after being em-

bedded in paraffin and the sections were stained with hematoxylin & eosin (H&E) for histopathological examination by Ts2R microscope (Nikon Vison Co., Ltd., Tokyo, Japan).

The right proximal femurs were performed a Micro-CT analysis by Quantum GX Micro-CT imaging system (PerkinElmer Co., Ltd., USA) at a high resolution. The scanning system was set to 90 kV, 88 μA and 72 μm of voxel size. A morphometric analysis of interest bone, which was extracted from the stack of cross-sectional images, was measured by CT analyzer. The 3D and 2D images were obtained for visualization and display. To evaluate the alterations in structural properties, the acquired images were calculated. Bone morphometric parameters were obtained by analyzing the volume of interest bone, including the bone mineral density (BMD), bone volume over tissue volume (BV/TV), trabecular number (Tb.N), trabecular thickness (Tb.Th), trabecular separation (Th.Sp), and structure model index (SMI).

GC-MS-based metabolomics

Sample preparation

A 50 μL aliquot of serum in an Eppendorf tube was added 200 μL methanol containing 10 μL internal standard (2-isopropylmalic acid, 1 mg·mL^{-1}) to deproteinize. The mixture was vortexed for 5 min before centrifuged at 1 3000 r·min^{-1} for 10 min at 4 °C. 200 μL of the supernatant was transferred to a clean Eppendorf tube and dried in a vacuum centrifuge concentrator before the subsequent derivatization. Quality control (QC) samples were prepared by pooling aliquots of all serum samples and were processed with the same procedure as that followed for the experiment samples.

For derivatization, 50 μL of methoxyamine hydrochloride in pyridine (15 mg·mL^{-1}) was added to the residue, being derivatized at 60 °C for 1 h. Then, each sample was added to 60 μL of MSTFA and heated at 70 °C for 1 h. After that, the sample was cooled to room temperature, centrifuged at 13 000 r·min^{-1} for 10 min prior to GC-MS analysis.

GC-MS analysis

GC-MS analysis was slightly modified as described in previously study [20]. Each 1 μL of derivatized sample was injected into an Agilent 7890B series gas chromatograph (Agilent Technologies, Germany) in split mode coupled with an Agilent 5977A series mass spectrometer (Agilent Technologies, Germany), equipped with a HP-5MS capillary column (30 m × 0.25 mm, i.d., 0.25 μm film thickness; Agilent J&W Scientific, Folsom, CA, USA). Helium was used as the carrier gas with a constant flow rate of 1 mL·min^{-1}; split ratio was 20 : 1. The column initial temperature was kept at 70 °C for 2 min, and then raised to 300 °C at the rate of 10 °C/min. The temperature was isothermally maintained at 300 °C for 5 min. The temperatures of the transfer line, ion source and quadrupole were 280, 250 and 150 °C, respectively. The mass spectra were obtained with electron ionization (70 eV) at full scan mode (*m/z* 50–600) with 5 min of solvent delay.

To monitor the data quality and process variation, QC samples containing aliquots from samples of all participating subjects were parallel-processed and intermittently injected throughout all the runs.

Multivariate statistical analysis

All GC-MS data was processed using Mass Profiler Professional (Agilent Technologies, Germany) for normalized as described in previous study [21]. SIMCA 14.1 (Umetrics, Sweden) was for multivariate statistical analysis. Partial least squares discriminant analysis (PLS-DA) and supervised orthogonal partial least squares discriminant analysis (OPLS-DA) were used to process the acquired data from the GC-MS analysis. After the multivariate statistical analysis, major metabolites were positively identified by comparing the mass spectra and retention times with those of standard compounds based on databases from the NIST 11.0 (Gaithersburg, MD, USA) mass spectral database with a similarity of more than 70%. Metabolites with a variable importance projection (VIP) value greater than 1.0 and a *P*-value less than 0.05 were selected as potential biomarkers, each related to a different group. The p-values for different metabolite-based cluster groups were determined using SPSS. Experimental groups were compared using one-way ANOVA and Duncan's test, with *P*-values < 0.05 considered significant.

Data processing

SPSS (Version 19) was for univariate data analysis. All biochemical data are expressed as means ± SD, and statistical analyses were performed using Student's *t*-test for independent two-sample and one-way ANOVA for the comparison of multiple means. $P < 0.05$ indicated statistical significance.

Results

Both CR and CH showed no-estrogen like effects

The mean of relative uterus weight was dramatically decreased by bilateral ovariectomy ($P < 0.001$), indicating that OVX model was successfully developed. CR or CH treatment did not increase uterus weight, compared with the OVX group ($P > 0.05$) (Fig. 1A). E2 level of administration groups showed no significant differences compared with OVX group ($P < 0.001$) (Fig. 1B). After 12 weeks, body weight had a representative change tendency during the whole experiment period (Fig. 1C), while the weight gain was prevented by CH or CR administration at sacrifice (Fig. 1D), compared with OVX group ($P < 0.001$). Moreover, under microscopy, the uterus of OVX rats decreased significantly in total mucosa and the percentages of uterine glands in the mucosa (Fig. 1E). There were no proliferation of endometrium and no change in uterine glands compared with OVX in treatment with CR or CH.

Comparison of anti-hyperlipemia effects between CR and CH

After 12 weeks, clinical chemistry results indicated that OVX caused significant elevation of TC, TG and LDL together with level decreases for HDL in rat serum compared with Sham groups (Fig. 2A). Treatments with CH or CR reversed these changes to various degrees, which were highlighted by significant decrease of TC, TG, LDL levels and increase of HDL levels compared with OVX rats. Lipid pro-

file analysis showed that there was no marked difference in TC and HDL levels among CH-L, CH-H, CR and Sham groups ($P > 0.05$). CH-L rats, however, exhibited higher TG and LDL levels than CR rats ($P < 0.05$). No difference was found in serum TG and LDL levels among CH-H, CR and Sham rats. The mean diameters of adipocyte in OVX rats were increased significantly, while CR or CH treatment made adipocytes smaller (Fig. 2B).

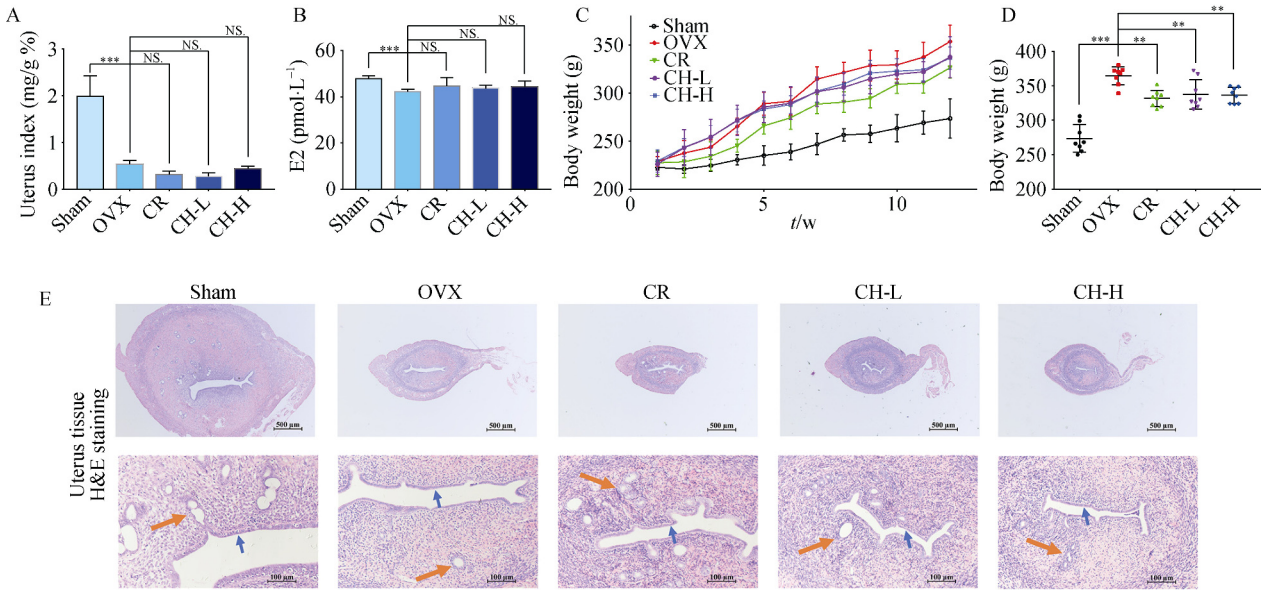

Fig. 1 Uterus relative weights (% of body weight) (A), estrogen levels (B), body weight trends (C), body weight at sacrifice (D), Uterus pathohistological sections (E). * Represents a significant difference from the OVX group. $^{*}P < 0.05$, $^{**}P < 0.01$, $^{***}P < 0.001$, (NS., no significant deference) $P > 0.05$. ↑in orange represents uterine glands; ↑ in blue represents endometrium

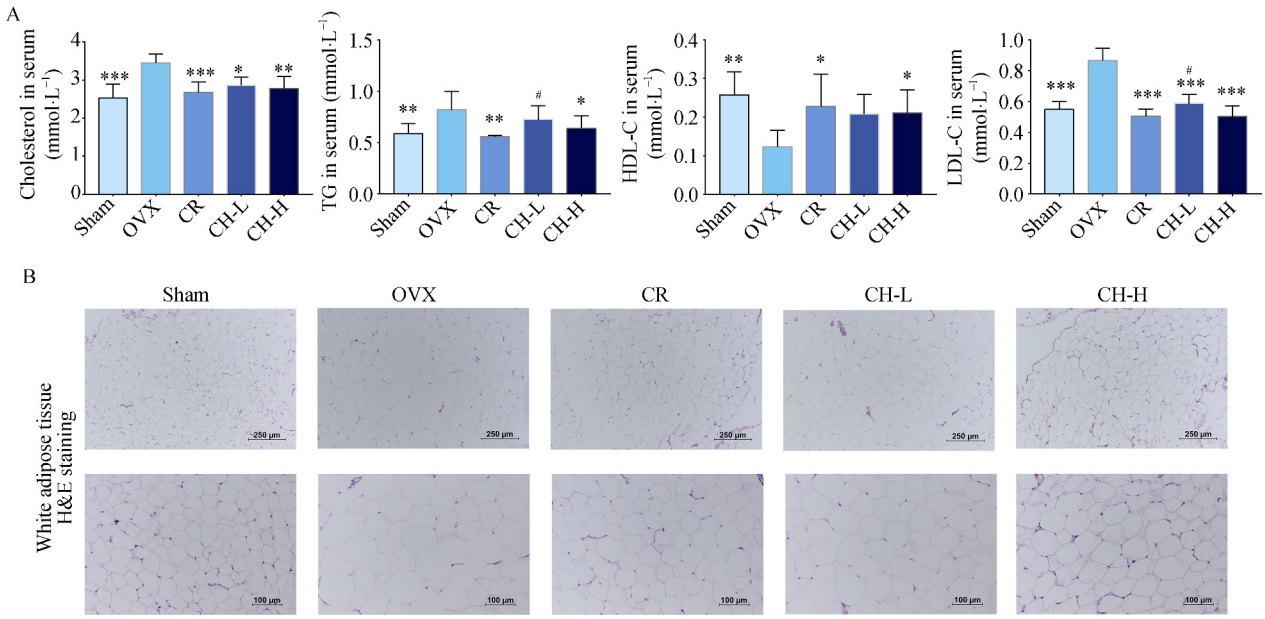

Fig. 2 Blood fat parameters (A) and abdominal fat pads pathohistological sections (B). * Represents a significant difference from the OVX group. $^{*}P < 0.05$, $^{**}P < 0.01$, $^{***}P < 0.001$,; $^{\#}$ Represents a significant difference from the CR group. $^{\#}P < 0.05$

Comparison of anti-osteoporosis effects between CR and CH

Bone turnover markers indicated that OVX caused significant elevation of ALP, OC, CTX-Ⅰ and TRACP 5b compared with Sham group ($P < 0.001$) (Fig. 3A). CR or CH administration could restore the levels of these parameters to normal status as Sham group, and there was no significant difference among CH-L, CH-H, CR and Sham groups ($P > 0.05$). 12 weeks after OVX, significant decrease in BMD values for the femur was observed ($P < 0.0001$). The BMD of the administrated rats was significantly higher than that in the OVX rats ($P < 0.001$). The levels of BV/TV, Tb.Th and Tb.N were higher in CR and CH groups than those in OVX rats

(Fig. 3B). In contrast, the parameters Tb.Sp and SMI were lower in CR and CH groups. Compared with CH-L, CH-H showed better effect in anti-osteoporosis, indicating dose-dependent recovery. However, no statistical differences were observed in Tb.N of rats treated with CH-L, as well as in BV/TV of rats treated with CR and CH-L when compared with OVX group. Additionally, in the pathological sections of trabecular bone (Fig. 4A) as well as three-dimensional (3D) and micro-CT two-dimensional (2D) images of the trabecular bone and cortical bone (Fig. 4B), the trabecular bone of OVX rats withered and became separated, while it was a well-connected network in Sham group. However, CR or CH could partly prevent the OVX-induced bone loss and improved the trabecular bone mass, trabecular separation and microarchitecture after 12 weeks of treatment.

Analysis for serum metabolomics profiles

The representative total ion current (TIC) chromatograms from OVX, Sham, CR, CH-L and CH-H groups were produced by GC-MS analysis. In order to examine whether the OVX modeling disordered the metabolic functions of rats as well as whether the treatments alleviated the disorder, PLS-DA analytical models were constructed. The value of R^2Y and Q^2 were 0.988 and 0.807, respectively, revealing the PLS-DA model was established successfully. In the PLS-DA diagrams, the OVX group and Sham group score plots were separated in two clusters. This pattern strongly indicated that endogenous metabolites in these two groups were significantly different. Moreover, the treatment of CH and CR restored the OVX metabolic disorder to varying degrees, with the score plots of administration groups and Sham group exhibited an overlap.

In order to find the differences in metabolic changes induced by CR or CH, pair-wise comparative OPLS-DA model was constructed. The distinct separations between OVX and Sham group, OVX and CR group, OVX and CH-L group, as well as OVX and CH-H group indicated endogenous metabolites were altered to varied degrees. Also, the parameters R^2Y (cum) and Q^2 (cum) value were considered to be a good fitness and predictability of the constructed OPLS-DA model, respectively. To avoid overfitting and validate the model, permutation test (n = 200) was necessary. All permuted R^2 and Q^2 values on the left were lower than the original point on the right, and the Q^2 regression line in blue had a negative intercept, suggesting the validity and robustness of all the OPLS-DA models.

The reproducibility of analysis was assessed by using QC samples which were analyzed after every 10 samples. 86% of differential metabolites had a relative standard deviation (RSDs) less than 30%. Based on these results, the high-quality data were sufficient to warrant further statistical analysis of the results to detect biomarkers.

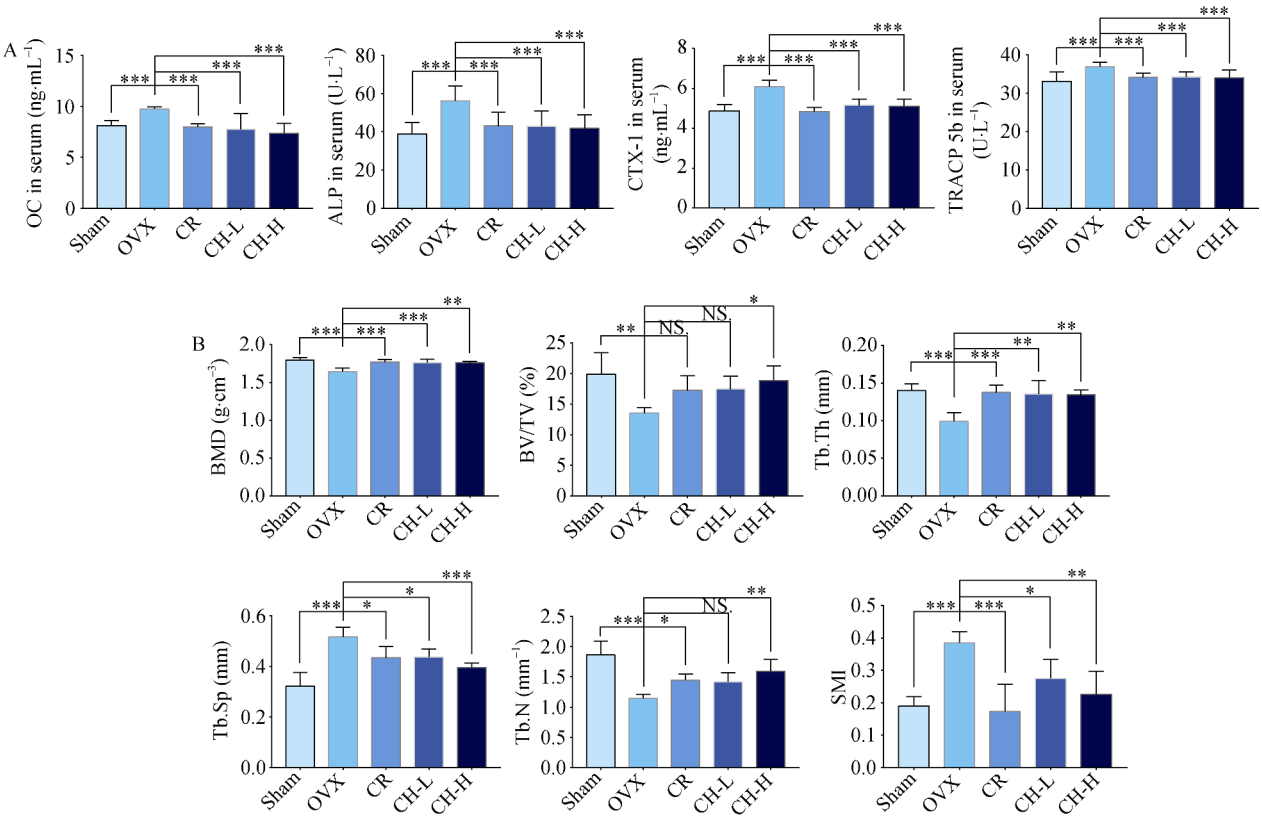

Fig. 3 Bone turnover marker (A), bone morphometric parameters (B). *Represents a significant difference from the OVX group. *$P < 0.05$, **$P < 0.01$, ***$P < 0.001$, (NS., no significant deference) $P > 0.05$

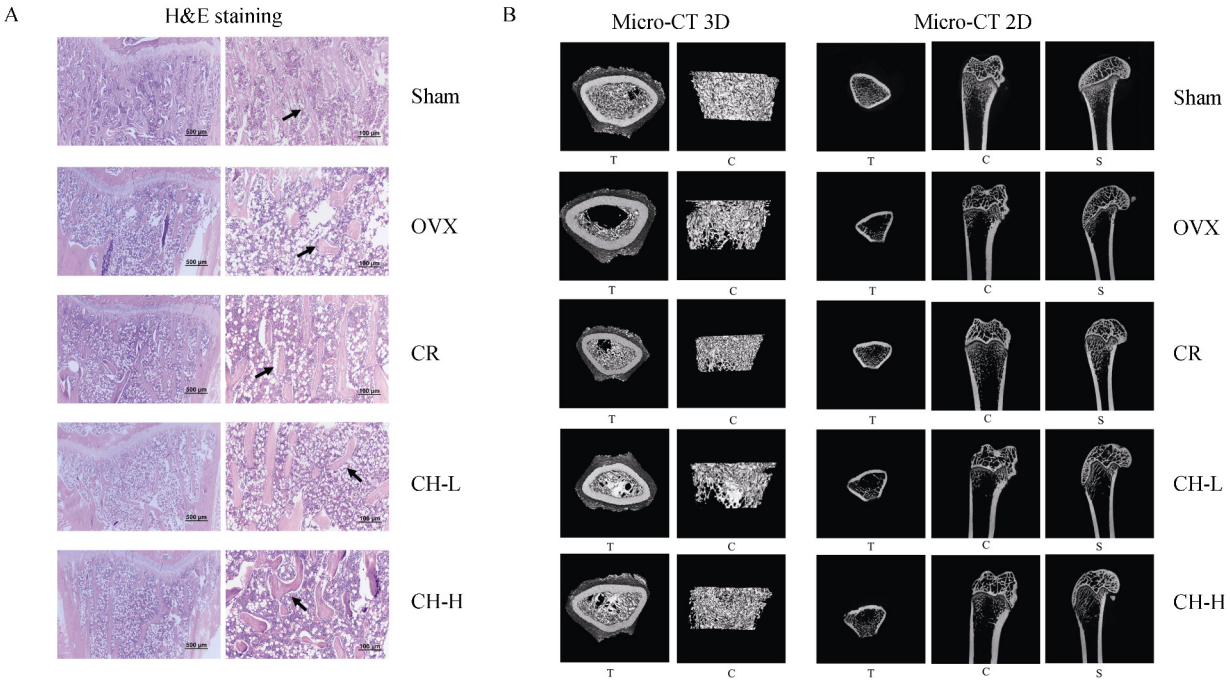

Fig. 4 Femur histopathology (A) and Micro-CT 2D & 3D model (B). ↑represents trabecular bone. T = transverse plane; C = coronal plane; S = sagittal plane

Identification of differential metabolites

Pair-wise comparative OPLS-DA was applied to distinguish the differences in chromatographic profiles in order to further uncover detailed metabolic changes induced by ovariectomy and the aforementioned treatments. Those metabolites satisfied the following two criteria: 1) VIP > 1.0, 2) $P < 0.05$, were selected. In this study, we were not only mainly interested in those metabolites changed in the status of OVX, but also took note of the metabolites which could be affected by CR or CH. Thus, a total of 20 different metabolites were identified (Table 1). Amino acids, organic acids, saccharides and fatty acids were identified as the discriminating metabolites, which indicated that these metabolites play an important role in the metabolic changes caused by OVX.

Table 1 GC-MS analysis of significantly altered serum metabolites of OVX rats administered with CH or CR

No.	RT[a)]	Metabolites	Formula	TMS [c)]	Log$_2$ (Fold change) [b)]				KEGG
					OVX/Sham	CR/OVX	CH-L/OVX	CH-H/OVX	
1	6.32	L-Lactic acid	$C_3H_6O_3$	2	5.934	–5.568	–5.236	–4.580	C00186
2	7.52	Oxalic acid	$C_2H_2O_4$	2	–1.813	2.084	5.765	2.125	C00209
3	7.79	Hydroxybutyric acid	$C_4H_8O_3$	2	13.909	–13.354	13.909	10.973	C00989
4	9.00	Urea	CH_4N_2O	2	12.468	–14.472	–4.819	–6.698	C00086
5	9.49	Glycerol	$C_3H_8O_3$	1	11.923	–13.927	0.433	–12.591	C00116
6	10.51	Glycine	$C_2H_5NO_2$	2	–4.860	7.631	10.811	2.410	C00037
7	12.15	L-Lysine	$C_6H_{14}N_2O_2$	3	4.405	–3.463	1.771	–3.277	C00047
8	12.74	L-Proline	$C_5H_9NO_2$	1	5.875	–2.809	–2.276	–8.793	C00148
9	13.17	Creatinine	$C_4H_7N_3O$	3	5.881	–8.279	–1.439	–5.426	C00791
10	13.88	L-Glutamic acid	$C_5H_9NO_4$	3	4.674	–4.891	–2.850	–4.608	C00025
11	13.97	L-Phenylalanine	$C_9H_{11}NO_2$	2	–5.812	5.729	5.024	5.440	C00079
12	15.60	L-Glutamine	$C_5H_{10}N_2O_3$	1	–4.063	4.187	3.161	4.142	C00064
13	17.09	D-Glucose	$C_6H_{12}O_6$	5	–4.195	4.317	7.660	4.144	C00031
14	19.55	L-Tryptophan	$C_{11}H_{12}N_2O_2$	2	7.002	0.831	3.942	–0.834	C00078

Continued

No.	RT[a)]	Metabolites	Formula	TMS [c)]	Log$_2$ (Fold change) [b)]				KEGG
					OVX/Sham	CR/OVX	CH-L/OVX	CH-H/OVX	
15	19.98	Stearic acid	$C_{18}H_{36}O_2$	2	–2.189	0.9303	1.576	1.051	C01530
16	21.09	Arachidonic acid	$C_{20}H_{32}O_2$	1	–6.553	6.626	2.084	6.867	C00219
17	21.81	Myo-Inositol	$C_6H_{12}0_6$	6	–4.529	4.722	8.628	4.730	C00137
18	22.83	Palmitic acid	$C_{16}H_{32}O_2$	2	–5.803	7.145	9.209	2.125	C00249
19	27.28	Cholesterol	$C_{27}H_{46}O$	1	–0.527	–1.662	4.881	1.118	C00187
20	27.59	Alpha-Linolenic acid	$C_{18}H_{30}O_2$	2	–11.923	6.155	9.393	12.591	C06427

Metabolites selected by VIP > 1.0 and $P < 0.05$ from OPLS-DA model;
a) Retention time (min); b) Relative levels of metabolites were converted into log$_2$ (fold-changes); c) Trimethylsilyl

In order to observe the trend of changes in metabolite concentrations, heatmaps were produced based on the relative amounts of each marker (Fig. 5A). Heatmaps revealed that OVX-induced clear decrease in the level of glycine, alpha-linolenic acid, hydroxybutyric acid and palmitic acid accompanied with elevation of L-tryptophan, myo-Inositol, arachidonic acid, L-glutamine, L-lysine, L-phenylalanine, stearic acid, L-proline, cholesterol, oxalic acid, creatinine, D-glucose, glutamic acid, L-lactic acid, urea and glycerol. Such changes were reversed to various extents by treatments with CH or CR. After CH-L treatment, the concentration of 15 of these 20 metabolites returned to normal, while all metabolites of these in CH-H or CR treatment were returned to normal. Meanwhile, a hierarchical cluster (HCL) was also performed, which is a task of grouping objects according to the similarity (Fig. 5A). As seen in the diagram, CH-H and CR were cross together and cluster with Sham group. Meanwhile, CH-L were also cluster with Sham group, but a little further than CH-H and CR group. Apparently OVX were far apart to these four groups, indicating that endogenous metabolites in OVX group were significantly different. In addition, HCL clustering results were consistent with PLS-DA score plots.

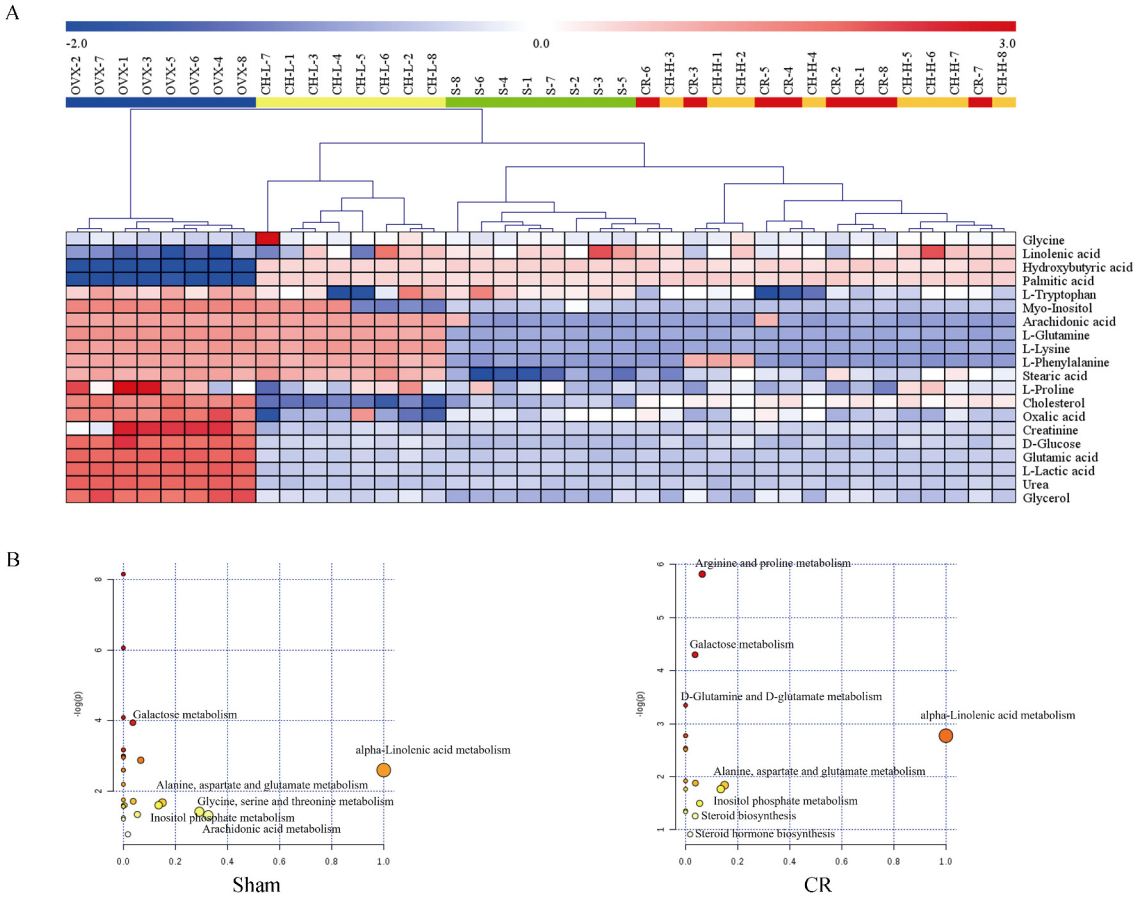

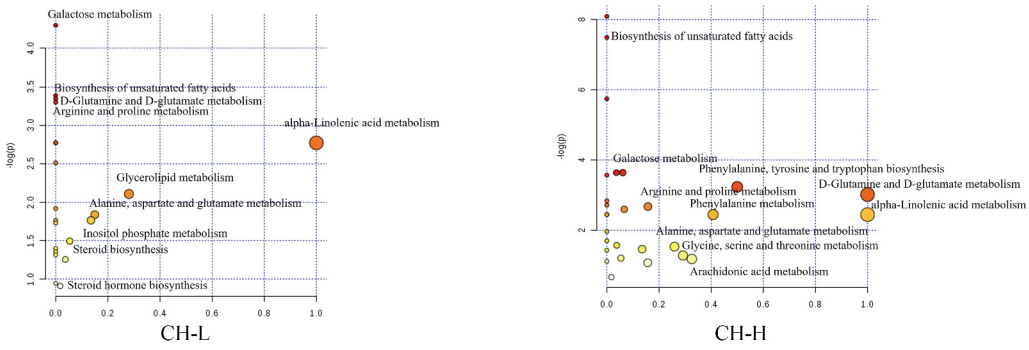

Fig. 5 Heatmaps visualization and HCL of the differential metabolites (A) and pathway impact based on the differential metabolites (B)

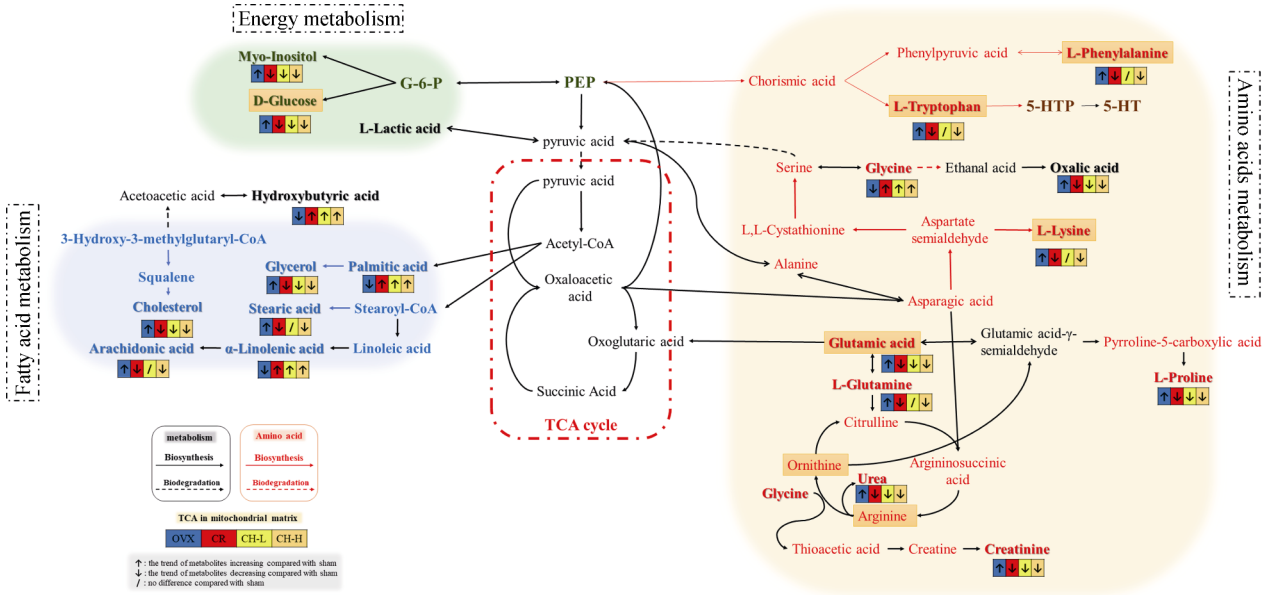

Fig. 6 Metabolic pathway networks of significantly different metabolites

Metabolic pathway analysis

MetaboAnalyst 4.0 (http: //www.metaboanalyst.ca) was a web-based server, supporting further analysis which integrated enrichment analysis and pathway topology analysis. In order to get more information on these metabolites, the identified metabolites information for each compared group was then imported into MetaboAnalyst 4.0 (Fig. 5B). Pathways with impact values above 0.10 were regarded as significant. Serum metabolites of OVX group VS Sham group generated 10 metabolite pathways, alpha-linolenic acid metabolism showed the highest impact (1.0) among these pathways. There were 13 same metabolism pathways among CR, CH-L, CH-H and Sham group. Among these 13 pathways, alpha-linolenic acid metabolism/D-glutamine and D-glutamate metabolism/alanine, aspartate and glutamate metabolism/steroid hormone biosynthesis/steroid biosynthesis /biosynthesis of unsaturated fatty acids/galactose metabolism/arginine and proline metabolism were shown important impacts (impact > 0.1). We found that alpha-linolenic acid metabolism pathway was thought to be involved in the most relevant pathway influenced by OVX with the impact value of 1.0 among all the treatment groups. Furthermore, a metabolic network of the Kyoto Encyclopedia of Genes and Genomes (KEGG, http: // www.kegg.jp) pathway database was constructed (Fig. 6).

Discussion

Effect on hyperlipidemia and osteoporosis

Recently, various studies have revealed that HRT may increase the risk of endometrial and breast cancers. Thus, the uterotropic activities of CR and CH were determined. Our results showed that there was no increase in uterus wet weight in treatment rats as well as uterine pathology showed no endometrial hyperplasia. Furthermore, the level of E2 was decreased significantly in OVX group compared with Sham group. But there was no difference between administration group and OVX group. These findings illustrated that no-estrogen like effects happened. Therefore, these two herbs showed their unique advantages in treating menopausal symptoms compared with HRT/ERT.

Moreover, it is generally recognized that a rapid decrease in estrogen secretion can bring about a hypothalamic-pituitary- ovarian (HPO) axis imbalance [22], which leads to increase of body mass, change of adipose tissue distribution, lipid metabolism disorders, and also an increased frequency of menopausal syndrome [1, 23-24].

In present study, CR or CH administration prevented the expansion of abdominal adipose tissue and reversed the elevation of body weights occurring in OVX rats. In order to prove CH could be used as a substitute of CR, the statistical analysis of lipid profile between CH and CR groups was conducted. As we expected, CH exhibited similar therapeutic effects in relieving menopausal symptoms. CH-L and CH-H possessed different potentials in treating the syndromes might be due to their different amounts of bioactive chemicals.

Nowadays, bone remodeling can be accurately assessed by bone turnover markers (BTM) assays in serum, which reflect either bone formation or bone resorption cell activities [25]. So, we further examined the bone formation markers like OC and ALP as well as bone resorption markers like TRACP 5b and CTX-Ⅰ. In epidemiological studies, high bone remodeling rates were associated with more severe forms of osteoporosis and high risk of fracture. Consistent with previous researches [17-18], OVX-induced osteoporosis exhibited high BTM in our study. However, both CR and CH attenuated the high bone remodeling and showed no significant difference in bone formation markers among CH, CR and Sham groups. Moreover, in order to evaluate the effect of CR or CH on osteoporosis more accurately, Micro-CT was employed for qualitative and quantitative study. The results of femur H&E observation were consistent with Micro-CT analysis, showing that CH or CR could decrease trabecular separation as well as increase the trabecular bone area in rat femur. The results further suggested the comparable efficacy of CH treatment with that of CR. To some extent, CH showed therapeutically similar effects to CR on anti-hyperlipemia and anti-osteoporosis.

Metabolomic patterns

Considering that metabolic disorders represent one of typical menopausal syndrome, monitoring metabolite compositional changes is thus performed as an important approach for estimating therapeutic efficacy. It is well known that GC-MS is a robust and unbiased approach in metabolomics study, by employing the easily accessible database of NIST. As a result, GC-MS serum metabolomics study revealed that CR and CH could reverse fatty acid, glucose and amino acid metabolism-related metabolites in OVX rats to normal levels.

Lipid metabolism

Based on metabolomic pattern, we found that all the administration groups had pronounced impacts on lipid metabolism pathways, especially in alpha-linolenic acid metabolism, fatty acid metabolism and biosynthesis of unsaturated fatty acids. It is reported that estrogen deficiency might cause a lower rate of β-oxidation of fatty acids and greater biosynthesis of fatty acids [26]. Among fatty acid metabolism, the levels of cholesterol, arachidonic acid and glycerol were increased in OVX rats, while alpha-linolenic acid and palmitic acid were decreased. In our study, the elevation of cholesterol, arachidonic acid and glycerol demonstrated that β-oxidation was inhibited in OVX rats and the increase of fatty acid metabolism further led to osteoporosis.

Besides, alpha-linolenic acid (ALA), the essential omega-3 fatty acid, is a type of polyunsaturated fatty acids (PUFAs), which can reduce lipid, blood pressure and inflammatory cardiovascular disease risk factors in menopausal women [27-28]. Various studies showed that menopause affects fatty acid metabolism and tissue PUFAs content due to estrogen deficiency. In present study, the level of ALA was decreased in OVX rats compared with Sham group. In addition, ALA could convert into the longer chain and less saturated fatty acids, such as arachidonic acid (AA; 20:4 ω-6). AA is an n-6 PUFA, which plays an important role in lipid metabolism and is also a precursor for several proinflammatory eicosanoids [29]. It has been reported that AA decreases the proliferation of primary human osteoblasts and osteoblast-like cells [30], also promotes osteoclast genesis by stimulating RANK-L expression and inhibits OPG secretion by osteoblasts [31] CR and CH might correct lipid abnormalities by increasing their synthesis of the shorter-chain n-3 PUFA like ALA.

The administration of CR and CH-H reversed the abnormal fatty acid metabolites to the levels of Sham group, while CH-L did not reverse the AA content. CH-H showed stronger anti-hyperlipemia and anti-osteoporosis effect than CH-L did. This phenomenon might be caused by the inhibition effect in the course of ALA transforming into AA. Additionally, CH alleviated OVX-induced lipid metabolism perturbations and its mechanism was similar to CR.

Energy metabolism

Moreover, lipid is the important source and storage of metabolic energy, but high level of circulating free fatty acids leads to increased insulin resistance [32]. When insulin resistance occurs, glucose catabolism will be limited, resulting in the accumulation of glucose and impacting the production of ATP [24]. Glucose is vital for various post-glycolytic pathways involving biosynthesis of fatty acids, cholesterol and amino acids. It has been reported that ovariectomy and estrogen deficiency can lead to the increase of glucose level, visceral adipose tissue and the decrease of energy expenditure [33]. The elevation of myo-inositol, D-glucose and L-lactic acid was observed in OVX rats, while CH or CR administration could reverse the elevation of these metabolites in present study. As we seen, OVX can increase abdominal fat deposition with adipocyte hypertrophy. CH or CR administration induced inhibitory activities in the hypertrophy of adipocytes may due to the inhibitory effects on glucose.

Furthermore, it has been reported that bone is a source of hormones for energy metabolism, insulin resistance, obesity and diabetes development, suggesting that energy metabolism and bone metabolism have a certain degree of mutual feedback [34]. There is a fact that the bone remodeling process requires a lot of energy, but once the energy metabolism is disturbed, the bone remodeling process will be seriously affected. Moreover, L-lactic acid is an important intermediate in the metabolism of organisms, and is closely related to glucose metabolism, lipid metabolism, protein metabolism and intracellular energy metabolism. L-lactic acid is also a crucial intermediate for the regulation of collagen biosynthesis during osteogenesis [35]. Therefore, the increased bone turnover formation associated with elevated L-lactic acid, resulted in low BMD in OVX rats.

It was shown that CR and CH administration attenuated energy metabolism-related metabolites in OVX-induced rats, thereby strengthening the ability of controlling glucose level in OVX rats. Thus, to an extent, energy metabolism disorders caused by OVX were reversed by CH or CR administration. In addition, CH exerted similar mechanism to CR for regulating multiple energy metabolites.

Amino acid metabolism

It has been reported that an optimal balance of amino acid circulation is vitally important, and menopause may contribute to future metabolic risk via influencing amino-acid concentrations [36]. The levels of amino acids such as L-glutamine, glutamic acid, L-lysine, and L-proline returned to Sham level by CR or CH treatment. Glutamine may regulate bone metabolism via osteoclasts and can interconvert to glutamate which leads to bone resorption via the expression of glutamate receptors on bone cells, especially osteoclasts [35]. This phenomenon could explain the association between elevated glutamine and low bone density. Moreover, the OVX-induced accumulation of serum proline might arise from the estrogen deficiency that causes the excitation of glutamic γ-semialdehyde dehydrogenase and deficiency of glutamic dehydrogenase [37]. Notably, different from CH-L, CH-H had pronounced impacts on phenylalanine metabolism and tryptophan metabolism. Phenylalanine and tryptophan are aromatic amino acids, which can interact with the calcium-sensing receptor (CaR) [38] and affect the body calcium metabolism and bone homeostasis. Phenylalanine is the biosynthesis precursors of important neurotransmitters, such as dopamine, epinephrine, thyroid hormones and norepinephrine [39]. If the biosynthesis pathway of neurotransmitters is disturbed, there will be accumulation of phenylalanine. Tryptophan is a precursor for serotonin, and the increase of which in the OVX model is due to the catabolism of tryptophan to alanine being blocked, and the hydroxylation of tryptophan was inhibition. Serotonin (5-HT) are the hydroxylated product of tryptophan and there is growing evidence that serotonin has been shown to increase bone mass by increasing the recruitment and proliferation of osteoblasts [40].

Conclusion

In summary, both CR and CH showed potential to alleviate menopause symptoms including hyperlipemia, osteoporosis and metabolic disorders, while without exhibiting estrogen-like effects. This work not only provides new insights into the herbal remedy of menopause, but also for the first time demonstrates that CH is therapeutically similar to CR in relieving menopausal symptoms. Hence, the medicinal value of CH serving as an alternative to CR deserves attention.

References

[1] Nelson HD. Menopause [J]. *Lancet*, 2008, **371**(9614): 760-770.
[2] Takahashi TA, Johnson KM. Menopause [J]. *Med Clin North Am*, 2015, **99**(3): 521-534.
[3] Go H, Ryuk JA, Lee HW, *et al.* Palmiwon attenuates hepatic lipid accumulation and hyperlipidemia in a menopausal rat model [J]. *Menopause*, 2015, **22**(8): 872-884.
[4] Tella SH, Gallagher JC. Prevention and treatment of postmenopausal osteoporosis [J]. *J Steroid Biochem Mol Biol*, 2014, **142**: 155-170.
[5] Gordon JL, Girdler SS. Hormone replacement therapy in the treatment of perimenopausal depression [J]. *Curr Psychiatry Rep*, 2014, **16**(12): 517.
[6] Beral V. Ovarian cancer and hormone replacement therapy in the Million Women Study [J]. *Lancet*, 2007, **369**(9574): 1703-1710.
[7] Bae JM, Kim EH. Hormone replacement therapy and risk of breast cancer in Korean women: a quantitative systematic review. [J]. *J Prev Med Public Health*, 2015, **48**(5): 225-230.
[8] Eden JA. Menopausal status, adipose tissue, and breast cancer risk: impact of estrogen replacement therapy [J]. *Horm Mol Biol Clin Investig*, 2013, **14**(2): 57-63.
[9] Bai W, Henneicke-von Zepelin HH, Wang S, *et al*. Efficacy and tolerability of a medicinal product containing an isopropanolic black cohosh extract in Chinese women with menopausal symptoms: a randomized, double blind, parallel-controlled study versus tibolone [J]. *Maturitas*, 2007, **58**(1): 31-41.
[10] Sun Y, Yu Q, Shen Q, *et al*. Black cohosh ameliorates metabolic disorders in female ovariectomized rats [J]. *Rejuvenation Res*, 2016, **19**(3): 204-214.
[11] Da YM, Niu KY, Liu SY, *et al*. Does *Cimicifuga racemosa* have the effects like estrogen on the sublingual gland in ovariectomized rats? [J]. *Biol Res*, 2017, **50**(1): 11.
[12] Leach MJ, Moore V. Black cohosh (*Cimicifuga* spp.) for menopausal symptoms [J]. *Cochrane Database Syst Rev*, 2012, **9**(9): CD007244.
[13] Merchant S, Stebbing J. Black cohosh, hot flushes, and breast cancer [J]. *Lancet Oncol*, 2015, **16**(2): 137-138.
[14] *Pharmacopoeia of The People's Republic of China* [S]. 2015: 73-74.
[15] Li JX, Liu J, He CC, *et al*. Triterpenoids from *Cimicifugae* rhizoma, a novel class of inhibitors on bone resorption and ovariectomy-induced bone loss [J]. *Maturitas*, 2007, **58**(1): 59-69.
[16] Ahn BS, Yang M, Jang H, *et al*. Evaluation of the antiosteoporotic potential of *Cimicifuga heracleifolia* in female mice. [J]. *Phytother Res*, 2012, **26**(5): 663-668.
[17] Jiang B, Ma C, Motley T, *et al*. Phytochemical fingerprinting to

thwart black cohosh adulteration: a 15 Actaea species analysis [J]. *Phytochem Anal*, 2011, **22**(4): 339-351.

[18] Li JX, Yu ZY. Cimicifugae rhizoma: from origins, bioactive constituents to clinical outcomes [J]. *Curr Med Chem*, 2006, **13**(24): 2927-2951.

[19] Ma C, Kavalier AR, Jiang B, *et al*. Metabolic profiling of Actaea species extracts using high performance liquid chromatography coupled with electrospray ionization time-of-flight mass spectrometry [J]. *J Chromatogr A*, 2011, **1218**(11): 1461-1476.

[20] Zhao DS, Jiang LL, Fan YX, *et al*. Investigation of Dioscorea Bulbifera Rhizome-induced hepatotoxicity in rats by a multi-sample integrated metabolomics approach [J]. *Chem Res Toxicol*, 2017, **30**(10): 1865-1873.

[21] Liu FJ, Liang D, Miao LY, *et al*. Liver-specific metabolomics characterizes the hepatoprotective effect of saponin-enriched Celosiae Semen extract on mice with nonalcoholic fatty liver disease [J]. *J Func Foods*, 2018, **42**: 185-194.

[22] Jayagopal V, Albertazzi P, Kilpatrick ES, *et al*. Beneficial effects of soy phytoestrogen intake in postmenopausal women with type 2 diabetes [J]. *Diabetes Care*, 2002, **25**(10): 1709-1714.

[23] Suliga E, Koziel D, Ciesla E, *et al*. Factors associated with adiposity, lipid profile disorders and the metabolic syndrome occurrence in premenopausal and postmenopausal women [J]. *PLoS One*, 2016, **11**(4): e0154511.

[24] Bendsen NT, Haugaard SB, Larsen TM, *et al*. Effect of trans-fatty acid intake on insulin sensitivity and intramuscular lipids—a randomized trial in overweight postmenopausal women [J]. *Metabolism*, 2011, **60**(7): 906-913.

[25] Lenora J, Ivaska KK, Gerdhem P. Use of bone turnover markers in osteoporosis [J]. *Clin Rev Bone Miner Metab*, 2009, **8**(1): 1-14.

[26] Ma B, Zhang Q, Wang GJ, *et al*. GC-TOF/MS-based metabolomic profiling of estrogen deficiency-induced obesity in ovariectomized rats [J]. *Acta Pharmacol Sin*, 2011, **32**(2): 270-278.

[27] Zhao G, Etherton TD, Martin KR, *et al*. Dietary alpha-linolenic acid inhibits proinflammatory cytokine production by peripheral blood mononuclear cells in hypercholesterolemic subjects [J]. *Am J Clin Nutr*, 2007, **85**(2): 385-391.

[28] Gortan Cappellari G, Losurdo P, Mazzucco S, *et al*. Treatment with n-3 polyunsaturated fatty acids reverses endothelial dysfunction and oxidative stress in experimental menopause [J]. *J Nutr Biochem*, 2013, **24**(1): 371-379.

[29] Lands WEM. Control of prostaglandin biosynthesis [J]. *Prog Lipid Res*, 1981, **20**: 875-883.

[30] Longo AB, Ward WE. PUFAs, Bone mineral density, and fragility fracture: findings from human studies. [J]. *Adv Nutr*, 2016, **7**(2): 299-312.

[31] Ma B, Liu J, Zhang Q, *et al*. Metabolomic profiles delineate signature metabolic shifts during estrogen deficiency-induced bone loss in rat by GC-TOF/MS [J]. *PLoS One*, 2013, **8**(2): e54965.

[32] Lin Y, Berg AH, Iyengar P, *et al*. The hyperglycemia-induced inflammatory response in adipocytes: the role of reactive oxygen species [J]. *J Biol Chem*, 2005, **280**(6): 4617-4626.

[33] Xue L, Wang Y, Liu L, *et al*. A HNMR-based metabonomics study of postmenopausal osteoporosis and intervention effects of Er-Xian Decoction in ovariectomized rats [J]. *Int J Mol Sci*, 2011, **12**(11): 7635-7651.

[34] Confavreux CB. Bone: from a reservoir of minerals to a regulator of energy metabolism [J]. *Kidney Int*, 2011, **79**: S14-S19.

[35] You YS, Lin CY, Liang HJ, *et al*. Association between the metabolome and low bone mineral density in Taiwanese women determined by ^{1}H NMR spectroscopy [J]. *J Bone Miner Res*, 2014, **29**(1): 212-222.

[36] Auro K, Joensuu A, Fischer K, *et al*. A metabolic view on menopause and ageing [J]. *Nat Commun*, 2014, **5**: 4708.

[37] Liu YR, Huang RQ, Xiao BK, *et al*. ^{1}H NMR metabolic profiling analysis offers evaluation of Nilestriol treatment in ovariectomised rats [J]. *Mol Cell Endocrinol*, 2014, **387**(1-2): 19-34.

[38] Conigrave AD, Brown EM, Rizzoli R. Dietary protein and bone health: roles of amino acid-sensing receptors in the control of calcium metabolism and bone homeostasis [J]. *Annu Rev Nutr*, 2008, **28**: 131-155.

[39] Zhang L, Wang Y, Xu Y, *et al*. Metabonomic analysis reveals efficient ameliorating effects of acupoint stimulations on the menopause-caused alterations in mammalian metabolism [J]. *Sci Rep*, 2014, **4**: 3641.

[40] Pernow Y, Thoren M, Saaf M, *et al*. Associations between amino acids and bone mineral density in men with idiopathic osteoporosis [J]. *Bone*, 2010, **47**(5): 959-965.

Cite this article as: MIAO Lan-Yun, CHU Thi Thanh Huyen, LI Ping, JIANG Yan, LI Hui-Jun. *Cimicifuga heracleifolia* is therapeutically similar to black cohosh in relieving menopausal symptoms: evidence from pharmacological and metabolomics studies [J]. *Chin J Nat Med*, 2019, **17**(6): 435-445.